Applied Catalysis B: Environmental 181 (2016) 769–778

Contents lists available at ScienceDirect

Applied Catalysis B: Environmental

journal homepage: www.elsevier.com/locate/apcatb

Ni–Al bimetallic catalysts for preparation of multiwalled carbon nanotubes from polypropylene: Influence of the ratio of Ni/Al

Yinlong Shen, Weiguang Gong*, Baicun Zheng*, Lei Gao

Research & Development Center for Sports Materials, East China University of Science and Technology, Shanghai 200237, PR China

ARTICLE INFO

Article history:
Received 9 June 2015
Received in revised form 24 August 2015
Accepted 30 August 2015
Available online 1 September 2015

Keywords:
Ni–Al
Bimetallic catalyst
Carbon nanotubes
Polypropylene

ABSTRACT

This study designed a novel Ni–Al bimetallic catalyst for preparation of multiwalled carbon nanotubes (MWCNTs) from polypropylene (PP). The study further investigated the influence of Al content on the catalytic activity of Ni catalyst. A series of bimetallic Ni–Al catalysts were prepared and then characterized by X-ray diffraction, N_2-adsorption–desorption isotherms, transmission electron microcopy and temperature programmed reduction analysis. It was found that bimetallic Ni–Al catalysts had higher surface area, higher reduction temperature, smaller Ni particle size and improved stability. Consequently, the addition of Al not only dramatically enhanced the yield of MWCNTs, but simultaneously improved the morphology and graphitization of MWCNTs. The activities of the bimetallic Ni–Al catalysts were dependent on their composition. Among the different Ni–Albimetallic catalysts, Ni–Al catalyst showed the highest activity when the ratio of Ni/Al was 9/1. Moreover, the obtained MWCNTs presented smooth surface with highest graphitization degree. The improvement of catalytic activity and stability obtained for bimetallic Ni–Al catalysts was attributed to an appropriate interaction and synergy between Ni species and amorphous Al_2O_3. The combined results indicate that the addition of Al to Ni catalyst with an appropriate amount of Al can give rise to a bimetallic catalyst with excellent properties for synthesis of MWCNTs from PP. With our bimetallic Ni–Al catalyst, it is promising to achieve mass production of MWCNTs by using waste polymers as feedstock.

1. Introduction

In the past few decades, carbon nanotubes (CNTs) have received intense research interests on account of their desirable mechanical, optical, electrical and thermal properties [1]. In general, methane [2–4], ethylene [5–7], acetylene [8–10] and other hydrocarbons have been used as carbon sources for CNT synthesis. Apart from these hydrocarbons, the use of waste polymers as feedstock is more environmental and economical for CNT synthesis. For the treatment of waste polymers, landfill and incineration are far from being widely accepted due to their related environmental pollution. Upcycling is the process of converting waste materials into something useful and more valuable [11–13]. Therefore, transforming waste polymers into high value-added CNTs is desirable. Recently, Zhuo et al. [14] have used stainless-steel wire mesh as both catalyst and substrate to synthesize multiwalled CNTs (MWCNTs) from polyethylene. However, the overall yield of MWCNTs was low. Mishra et al. [15] have used waste PP as a precursor to synthesize MWCNTs via chemical vapor deposition. However, these methods require complicated equipment, inert gas protection, and long reaction time. Hence, high-efficiency and low-cost conversion of waste polymer to MWCNTs remains challenging. Gong et al. [13,16–20] have developed a versatile method called flame synthesis to prepare MWCNTs and done a series of investigations on the preparation of carbon materials from polyolefins, and achieved many progresses in this field.

Efforts to achieve improvements in activity and stability of Ni-based catalysts for the formation of CNTs can be facilitated by the discovery of bi-/trimetallic Ni-based catalysts. Compared with the monometallic Ni catalyst, bi-/trimetallic Ni-based catalysts, which are relatively cheap, often show exceptional electronic and chemical properties [21], better catalytic performances [22], and higher stability [23]. Therefore, the Ni-based bi-/trimetallic catalysts have been widely used as an alternative to monometallic Ni catalysts in various catalytic reactions. Up to date, several Ni-based bi-/trimetallic catalysts have been investigated, such as Ni–Co [24–26], Ni–Mg [27], Ni–Cu [3,28], Ni–Mo [29–31], Ni–Cu–Co [32], Ni–Cu–Mo [33] and Ni–Mg–Al [34–36]. Fan et al. [24] have found that the Ni–Co bimetallic catalyst exhibited higher and more

* Corresponding authors.
E-mail addresses: gongwg@ecust.edu.cn (W. Gong), baicun@ecust.edu.cn (B. Zheng).

http://dx.doi.org/10.1016/j.apcatb.2015.08.051
0926-3373/

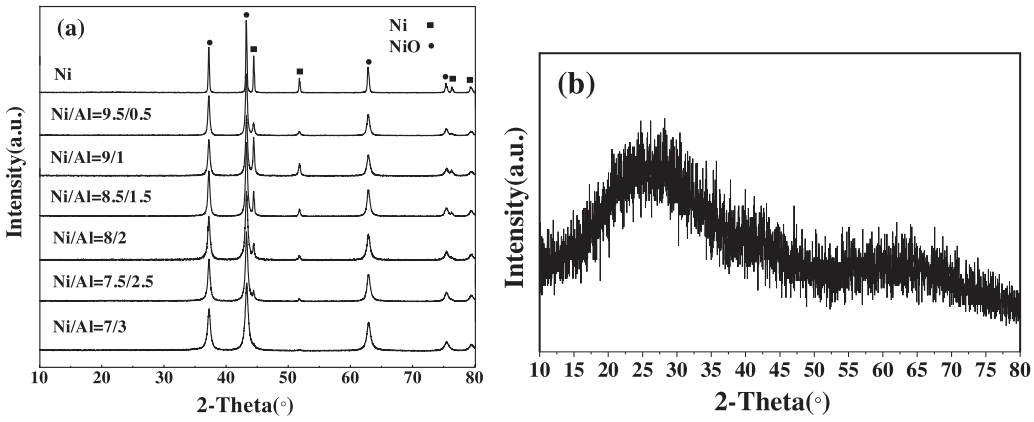

Fig. 1. XRD patterns of Ni and Ni–Al catalyst: (a) Ni and Ni–Al catalysts, and (b) Al_2O_3.

sustaining catalytic activity and excellent regeneration capability when compared with the monometallic catalyst. The advantage of the bimetallic catalyst usually stems from the better metal dispersion, smaller metal particle size and synergetic effect between Ni and Co particles. Kukushkin et al. [33] have investigated the influence of Mo on catalytic activity of Ni-based catalysts in hydrodeoxygenation of esters. It was found that an increase in the Mo content (from 0.0% to 6.9%) in the Ni–Cu–Mo/Al_2O_3 catalysts leads to an increase in the yield of normal alkanes. The XPS data showed that the increase in the conversion of fatty acid esters is related to changes in the ratio between different oxidation states of molybdenum (Mo^0, Mo^{4+}, and Mo^{6+}) on the surface of the Ni–Cu–Mo/Al_2O_3 catalysts.

Here, we develop bimetallic Ni–Al catalysts with excellent stability and superior activity for the synthesis of MWCNTs of PP by optimizing the composition of the bimetallic Ni–Al catalysts. The addition of Al not only dramatically increased the yield of MWCNTs (74.2 wt% versus 36.9 wt%), but simultaneously improved the morphology and graphitization degree of MWCNTs as well. The highest yield of MWCNTs was 85.5%. To our knowledge, this is the first time that Ni–Al bimetallic catalysts are used in the preparation of MWCNTs from polypropylene. This work presents feasibility of growing MWCNTs from polypropylene by using an efficient Ni–Al catalyst and highlights the potential of this approach for large-scale production of MWCNTs from waste polymers.

2. Experimental

2.1. Materials

Polypropylene (PP, trademark T30S) was purchased from Maoming petrochemical Corporation, China. PP-MAH (trademark 2901) was supplied by Shenzhen hualin Chemical Co., China. Organic-modified montmorillonite (OMMT, Nanolin DK4, organic modifier: Octadecyl Trimethyl Ammonium Bromide; 90 meq/g), and Na-MMT were supplied by Zhejiang Fenghong new material CO., China. The cation exchange capacity (CEC) of Na-MMT was 90 meq/100 g. $Ni(NO_3)_2{\cdot}6H_2O$, $Al(NO_3)_3{\cdot}9H_2O$ and polyethylene glycol (PEG, $M_w = 200$) with analytical grade quality were purchased from Lingfeng Chemical Company of Shanghai and used without further purification.

2.2. Preparation of Ni–Al catalyst and MWCNTs

$Ni(NO_3)_2{\cdot}6H_2O$ was dissolved in PEG, alone or together with $Al(NO_3)_3{\cdot}9H_2O$. The resultant solution was kept at 923 K for 10 min. The obtained material was grounded to powders, denoted as Ni catalyst and Ni–Al catalyst.

PP was then mixed with Ni–Al catalyst and OMMT in a Brabender mixer at 453 K for 10 min. The resultant samples were denoted as PP/PP-MAH/$_x$OMMT/$_y$Ni–Al, where x and y represented the amount of OMMT and Ni–Al catalyst, respectively.

Subsequently, the PP mixture was placed into a crucible with a cab. Then the crucible was sent to a muffle furnace at 1073 K for 8 min. Subsequently, the crucible was cooled to room temperature in dryer. The obtained residue was further purified with HF and HNO_3. The yield of MWCNTs was calculated by dividing the amount of the purified MWCNTs by the carbon element in the sample. Each measurement was repeated three times for reproducibility.

2.3. Characterization

The phase structure of Ni–Al catalysts and MWCNTs were analyzed by X-ray diffraction (XRD, Cu Kα radiation, λ = 1.5404 Å).

Temperature-programmed reduction (TPR) was performed in a quartz tube reactor, using a Micromeritics Chemisorb 2705 instrument. Fifty milligram of catalyst was placed in the reactor and reduced with a 5–95% N_2 (v/v) gas mixture. The temperature was increased to 973 K at a heating rate of 10 K/min.

The textural properties of Ni and Ni–Al catalysts were determined by N_2 absorption at 77 K using a Micromeritics ASAP 2020 instrument. The samples were outgassed in vacuum for 24 h at 200 °C before nitrogen absorption.

The morphologies of MWCNTs were examined by field-emission scanning electron microscopy (FE SEM, XL303SEM), transmission electron microscope (TEM, JEM-1400) and high-resolution transmission electron microscope (HRTEM, JEM-2100) at an accelerating voltage of 100 kV.

The vibrational properties of MWCNTs were characterized by a Renishaw 2000 model confocal microscopy Raman spectrometer using the 514.5 nm diode laser.

3. Results and discussion

3.1. Characterization of Ni and Ni–Al catalyst

First, wide-angle X-ray diffraction analysis was performed to confirm the composition of Ni and Ni–Al catalyst (Fig. 1). For both Ni catalyst and Ni–Al catalyst, well resolved peaks of nickel oxide at 37.2^0, 43.3^0, 62.9^0, 75.4^0 and 79.4^0 from (1 1 1), (2 0 0), (2 2 0), (3 1 1) and (2 2 2) planes, and metallic nickel at 44.5^0, 51.8^0, and 76.6^0 from (1 1 1), (2 0 0), and (2 2 0) planes respectively, were present. For Ni–Al bimetallic catalyst, the NiO and Ni average particle diameters on the basis of the full width at the half maximum (FWHM) of the NiO (012) and Ni (1 1 1) diffraction peaks using the Scherrer formula are given in Table 1. The average particle diameter of

Table 1
Particle size of NiO and Ni particles in the Ni–Al bimetallic catalysts and diameters of the obtained MWCNTs.

	Ni/Al = 9.5/0.5	Ni/Al = 9/1	Ni/Al = 8.5/1/5	Ni/Al = 8/2	Ni/Al = 7.5/2.5	Ni/Al = 7/3
NiO (nm)	25.9	24.9	24.8	23	23.4	20.9
Ni (nm)	31.0	25.9	33.2	30.1	30.3	
Diameter of MWCNTs (nm)	44.6	11.93	18.4	13.7	12.2	12.9
Length of MWCNTs (μm)	2–7	2–5	0.7–3	0.5–2	0.5–2	0.5–1.5

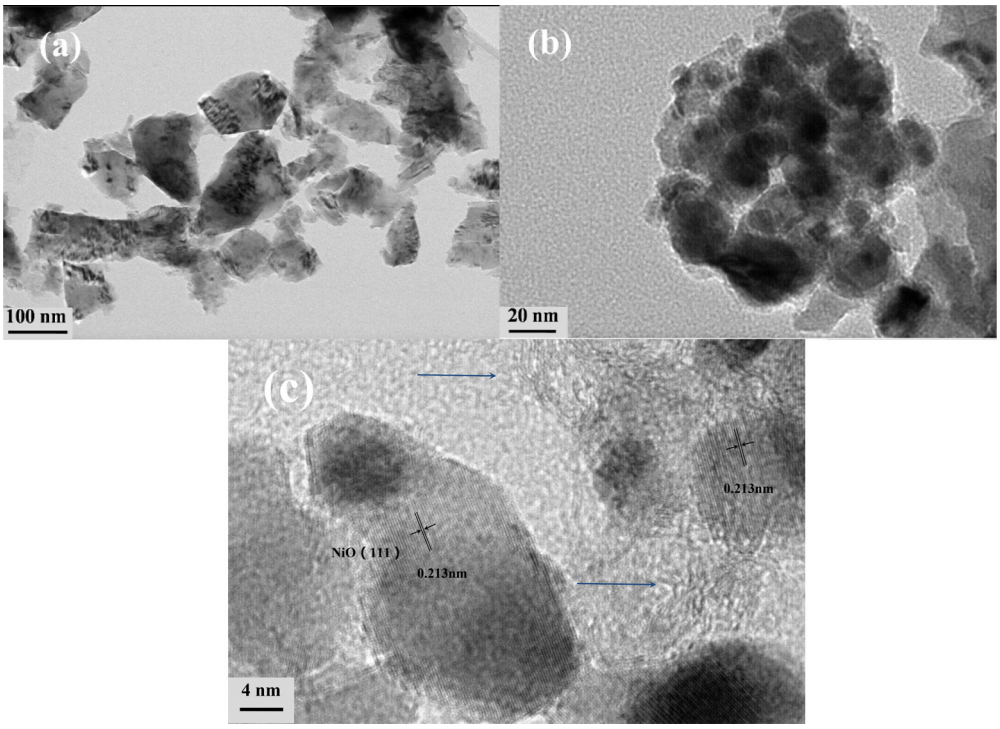

Fig. 2. TEM and HRTEM images of catalyst: (a) Ni catalyst, (b) Ni–Al catalyst (Ni/Al = 9/1), and (c) HRTEM for Ni–Al catalyst (Ni/Al = 9/1).

NiO was in the range of 20.9–25.9 nm and was found to decrease slightly with increasing Al loading. However, the same trend was not observed for Ni particle in the catalysts. Note that no peak representing Al based species were detected in Ni–Al catalyst. To figure out the state of Al based species, pure $Al(NO_3)_3{\cdot}9H_2O$ was used as precursor and amorphous Al_2O_3 was obtained under the same conditions (Fig. 1b).

Furthermore, information regarding the morphology of catalyst was obtained by TEM (Fig. 2). Ni catalyst displayed irregular shape with estimated sizes vary between 70 nm and 200 nm. In contrast, Ni–Al catalyst showed round shape with a mean diameter of 24.1 nm, which was in accordance with the XRD results. The TEM images showed that introducing Al into the Ni catalyst enabled the smaller size and uniform distribution of Ni nanoparticles. Furthermore, it was quite intriguing to find that the edge of NiO particles was wrapped by amorphous Al_2O_3 (see blue arrows in Fig. 2c). Al_2O_3 was mainly located at the boundary around NiO particle, and the D-spacing values of 0.213 nm corresponding to the (1 1 1) plane of NiO, as evident from the representative HRTEM images of Ni–Al bimetallic catalysts.

The reducibility of the non-promoted and Al-promoted Ni-based catalysts was studied using TPR (Fig. 3). Ni monometallic catalyst exhibited a pronounced reduction peak centered around 367 °C, which was assigned to the reduction of Ni^{2+} in the well-crystallized NiO phase [37,38]. The partial substitution of Ni by Al showed a strong influence in the TPR profile for all Ni–Al bimetallic catalysts. All the Ni–Al bimetallic catalysts showed single H_2 consumption domain of a broad peak ranging from 232°C to 675°C, but the peak maximum was shifted to higher temperature in comparison with that of Ni monometallic catalyst. Wu et al. [38] and Rivas et al. [37] have concluded that the shift of reduction temperature was attributed to Ni species strongly interacting with alumina. Zhang et al. [39] have concluded that Ni and Co may exist in the similar homogeneous oxide structure which leads to single-stage reduction with a broad peak. Therefore, the shift of reduction peak Ni–Al bimetallic sample to higher temperature was due to the increase of the NiO–Al_2O_3 interaction resulting from homogeneous Ni and Al oxide structure.

3.2. *Effect of the ratio of Ni/Al in the Ni–Al bimetallic catalysts on the yield of MWCNTs*

Fig. 4a depicts the yield of MWCNTs from PP/PP-MAH/$_{10}$OMMT/$_5$Ni–Al as a function of different ratio of Ni/Al. The yield of MWCNTs catalyzed by Ni catalyst was limited to only 36.9% without Al addition. The yield of MWCNTs jumped up dramatically to 74.2%, approximately twice of that observed for Ni catalyst, indicating a substantial enhancement in catalytic activity by the addition of Al. Then the yield remained relatively constant (until the ratio of Ni/Al reached 7:3), followed by a sharp decrease. Accordingly, the ratio of Ni/Al was fixed to 9/1 in the following experiments. The above results illustrated that the ratio of Ni/Al has a remarkable influence on the catalytic performance of Ni–Al bimetallic catalysts.

Next, we investigated the influence of the amount of Ni–Al catalyst on the yield of MWCNTs (Fig. 4b). For the PP/PP-

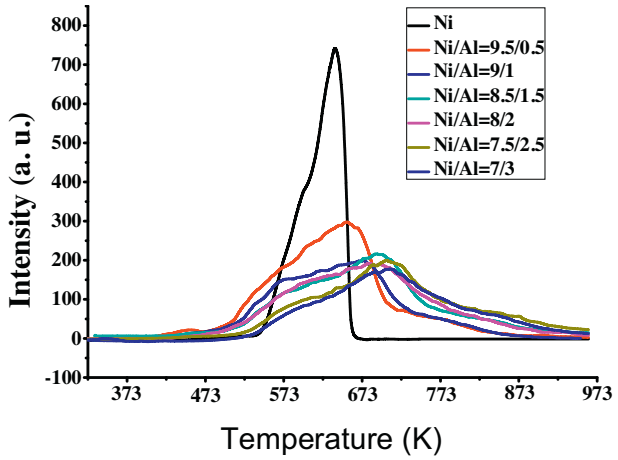

Fig. 3. TPR profiles of Ni and Ni–Al bimetallic catalysts.

MAH/$_{10}$OMMT/$_y$Ni–Al (Ni/Al = 9/1) mixture, the yield of MWCNTs rapidly increased to 73.5% when the catalyst was 5% and then slightly increased linearly up to 85.5% with rise in the amount of the catalyst. The highest yield of residue could be as high as 85.5%. The yield of MWCNTs showed high dependence on the ratio of Ni/Al and the amount of Ni–Al catalysts.

3.3. Effect of the ratio of Ni/Al in the Ni–Al bimetallic catalysts on the morphology and microstructure of MWCNTs

First, we compared the difference between MWCNTs catalyzed by Ni and Ni–Al bimetallic catalysts. The resultant residue catalyzed by Ni catalyst consisted of amorphous carbon and nonuniform MWCNTs (Figs. 5 and 6a). In contrast, as shown in Figs. 5 and 6, the obtained MWCNTs catalyzed by Ni–Al catalyst predominantly consisted of MWCNTs and had much narrower diameter distributions of MWCNTs. This observation illustrated that Al not only dramatically enhanced the catalytic activity of Ni catalysts towards the formation of MWCNTs, but simultaneously improved the morphology of MWCNTs.

Next, we investigated the influence of the ratio of Ni/Al in the Ni–Al bimetallic catalysts on the morphology using SEM. Interestingly, we observed a large amount of relatively straight and long MWCNTs when the ratio of Ni/Al was 9.5/0.5 and 9/1. However, the formed MWCNTs became shorter and winding when Al was further added, especially when the ratio of Ni/Al was 7/3. TEM observations were conducted to further clarify the effect of the amount of Al addition in the Ni–Al catalysts on the microstructure of MWCNTs (Fig. 6). The data of length and the average diameters are summarized in Table 1. An increased amount of Al in catalysts led to a substantial decrease in the length and diameter of MWCNTs, with a simultaneous deterioration of MWCNTs quality. To be specific, the length of MWCNTs decreased from approximately 5 μm to 0.5 μm, and the outer diameter declined from about 44.6 nm to 12.9 nm. For the quality of MWCNTs, the surface of MWCNTs seemed to be smooth when the content of Al was less than 10%. Further addition of Al made MWCNTs shorter and winding. What's more, HRTEM were conducted to further clarify the effect of the ratio of Ni/Al on the graphitization of MWCNTs. As shown in Fig. 7, the graphene layers in the MWCNTs obtained from Ni/Al ratio of 9/1 were parallel to the CNT axis. And the interlayer spacing between graphitic layers was about 0.34 nm, which was consistent with the ideal graphitic interlayer spacing. In contrast, when the ratio of Ni/Al was 7/3, the graphene layers of MWCNTs were oblique to the CNT axis at the angle of 20–25^0. Moreover, the interlayer spacing between graphitic layers was in the range of 0.34–0.36 nm, suggesting the low graphitization of MWCNTs when the ratio of Ni/Al was 7/3. The graphene layers were discontinuous and had more defects, and the surface of the MWCNTs was rugged. On the basis of HRTEM images, MWCNTs obtained from 9/1 had higher graphitization than those from 7/3. Therefore, we could conclude that the morphology and microstructure of MWCNTs are strongly affected by the ratio of Ni/Al.

3.4. Effect of the ratio of Ni/Al in the Ni–Al bimetallic catalysts on the graphitization of MWCN*Ts*

XRD patterns of the resultant MWCNTs after purification are displayed in Fig. 8a. Only two peaks characteristic of (0 0 2) and (1 0 1) reflections of graphite were observed. FWHM of diffraction peak of graphite (0 0 2) of MWCNTs catalyzed by Ni–Al catalyst was plotted as a function of the ratio of Ni/Al in Fig. 8b. FWHM showed a slight decline at the beginning, which exhibited a minimum of 0.487 before gradually increasing to 0.540 at increasing amount of Al in the Ni–Al bimetallic catalysts. The larger FWHM indicates that MWCNTs contains more defects and distortion when more Al is added [40], which is in line with TEM observations (Fig. 6). When the ratio of Ni/Al was 9/1, the obtained MWCNTs from PP/PP-MAH/$_5$OMMT/$_5$Ni–Al was of the highest graphitization and best quality. Furthermore, FWHM of the MWCNTs obtained from PP/PP-MAH/$_5$OMMT/$_5$Ni was higher than that of MWCNTs catalyzed by Ni–Al catalyst (~0.569 versus <0.540), reflecting that Al could improve the graphitization degree of MWCNTs.

Raman signals respectively at 1350 cm^{-1} and 1580 cm^{-1} are assigned to graphite D and G bands of MWCNTs. The relative intensity of G and D band (I_G/I_D) reflects the degree of structural ordering for the graphite sheets [41,42]. As can be calculated from the Raman spectrum in Fig. 9a, the I_G/I_D for the resultant MWCNTs is displayed as a function of the ratio of Ni/Al in Fig. 9b. The I_G/I_D increased with increasing amount of Al in bimetallic catalysts followed by a decline, showing a downward parabola. When Al addition was 10%, the resultant MWCNTs had minimum amount

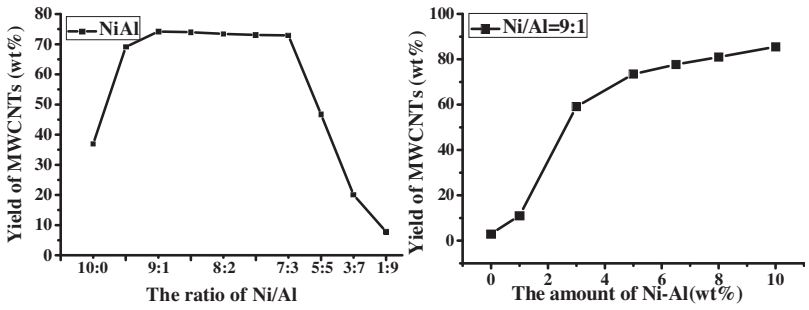

Fig. 4. Effect of various parameters on the yield of MWCNTs from PP/PP-MAH/OMMT/Ni–Al mixture at 1073 K: (a) the ratio of Ni/Al in catalyst, and (b) the amount of Ni–Al catalyst.

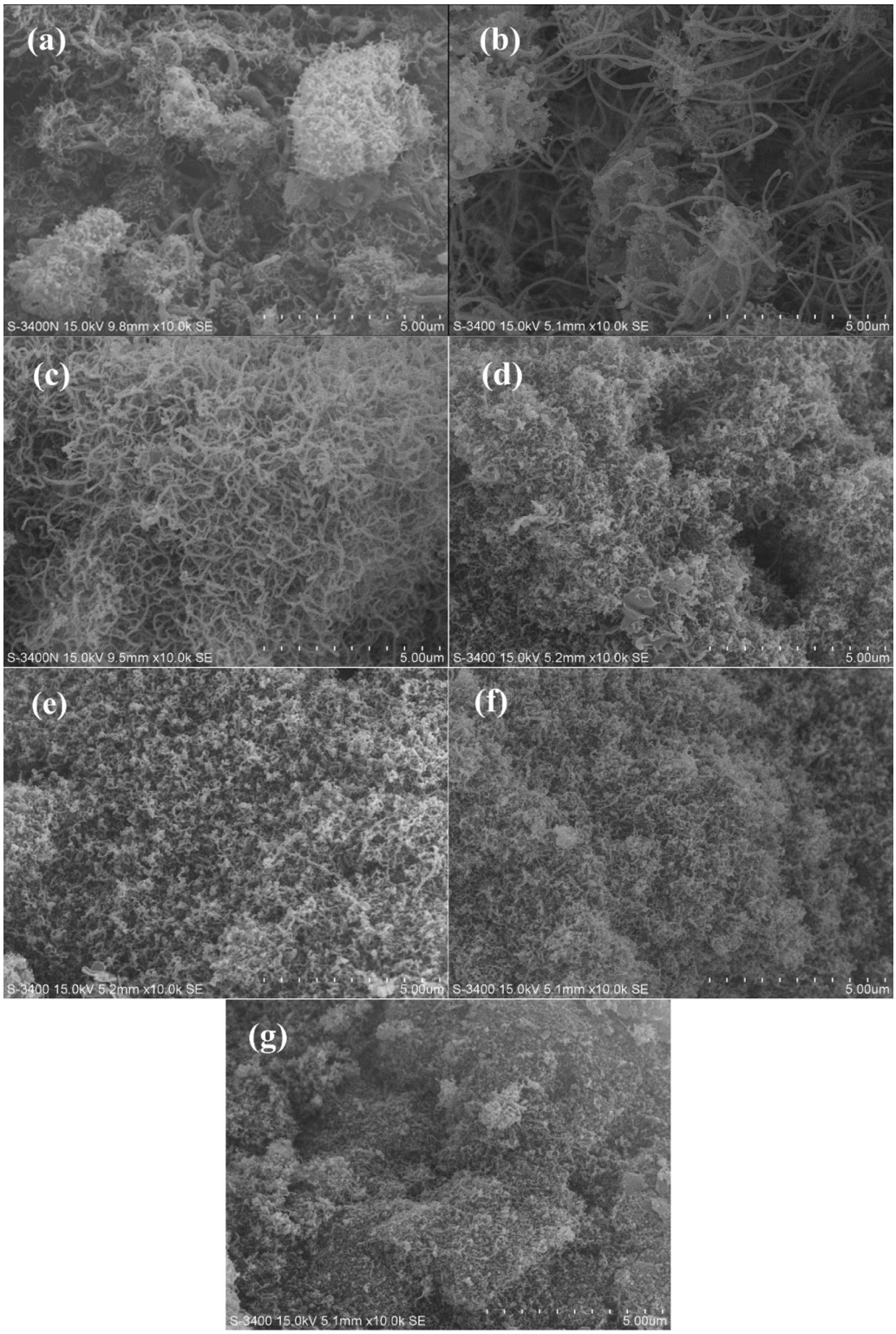

Fig. 5. Typical SEM images of residue char without purification from PP/PP-MAH/$_5$OMMT/$_5$Ni and Ni–Al catalyst mixture at 1073 K: (a) Ni, (b) Ni/Al = 9.5/0.5, (c) Ni/Al = 9/1, (d) Ni/Al = 8.5/1.5, (e) Ni/Al = 8/2, (f) Ni/Al = 7.5/2.5, and (g) Ni/Al = 7/3.

of defects inside the graphite sheets, in agreement with the TEM and XRD results. Moreover, the I_G/I_D of MWCNTs by Ni–Al catalysts was higher in comparison with that of Ni catalyst, which also reflected MWCNTs by Ni–Al catalyst had higher graphitization.

3.5. Discussion

Tang and his collegues [43,44] have put forward the possible process and mechanism for the growth of MWCNTs from PP by combination of OMMT and Nickel. The catalytic carbonization of

PP into MWCNTs can be divided into three steps: (1) At 473–573 K, alkyl ammonium in the OMMT firstly decomposes to form Br⊘nsted acid sites. Then the surface of PP mixture subsequently degrades in catalytic way, resulting in the production of light hydrocarbons and hydrogen which reduce NiO into metallic Ni. (2) Hydrocarbons deposit on the surface of Ni particle and further decompose into carbon atoms and hydrogen. These carbon atoms gradually absorb on Ni particle and diffuse, causing the distortion of Ni particle [45–47]. (3) These carbon atoms connect with each other to form dimers and trimmers. Subsequently, pentagons and hexagons form on the surface, which eventually interconnect so as to form graphite sheets. Then MWCNTs continue to grow with the further deposition and diffusion of carbon atoms.

What's more, it's of paramount importance to figure out why the addition of Al could enhance the catalytic activity of Ni catalyst. The significant improvement in yield of MWCNTs and improved morphology and quality of MWCNTs by Ni–Al bimetallic catalysts is more likely due to combined factors. First, the diameter of Ni catalyst varied between 70 nm and 200 nm, much larger than 24.1 nm of Ni–Al catalyst (TEM images in Fig. 2). According to previous report [48], the crystal size of Ni particle has a striking influence on the growth of carbon nanofibers (CNFs). Small Ni crystal yields a low growth rate and fast deactivation and thus a low final yield of CNF. And large Ni crystals reduce the growth rate because of low surface area. An optimum growth rate and yield of CNFs can be achieved on optimally sized Ni crystals. Therefore, the diameter range of 20.9–24.9 nm may locate in the optimum size range, thus resulting in much higher catalytic activity. Moreover, the addition of Al led to higher reduction temperature as shown by TPR results (Fig. 3). This enhancement in reduction temperature was more likely due to an appropriate interaction between NiO, Ni^0 and amorphous Al_2O_3. This interaction could significantly improve the catalytic activity of Ni-based catalyst. To prove that, we used a simple mixture of monometallic Ni catalyst and amorphous Al_2O_3

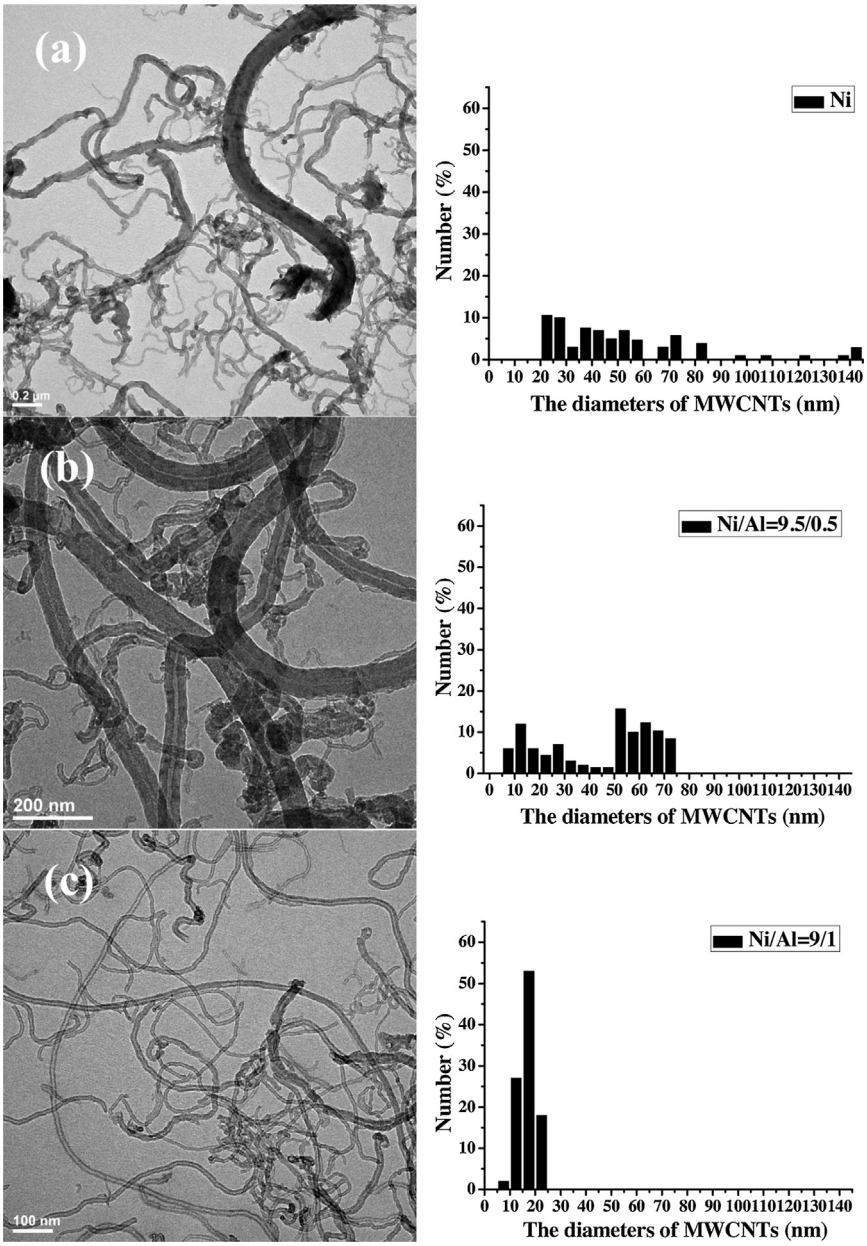

Fig. 6. Typical TEM images and particle size distribution histogram of MWCNTs from PP/PP-MAH/OMMT/Ni and Ni–Al catalyst mixture at 1073 K: (a) Ni, (b) Ni/Al = 9.5/0.5, (c) Ni/Al = 9/1, (d) Ni/Al = 8.5/1.5, (e) Ni/Al = 8/2, (f) Ni/Al = 7.5/2.5, and (g) Ni/Al = 7/3.

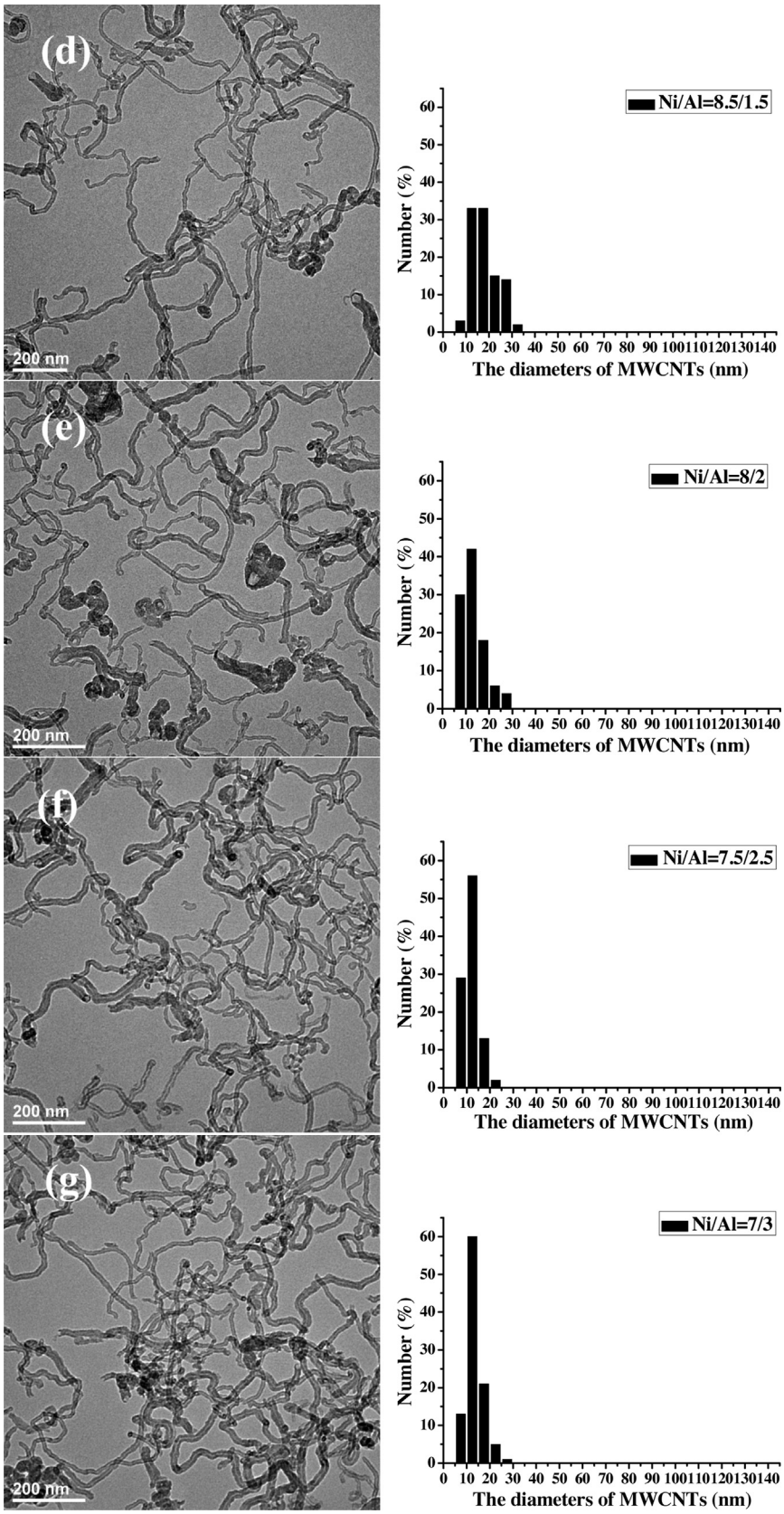

Fig. 6. (*Continued*).

to prepare MWCNTs. Surprisingly, the yield of MWCNTs was only 37.5 wt%. It was established that the synergy between Ni species and amorphous Al_2O_3 was a key factor to improve the catalytic activity of Ni catalyst.

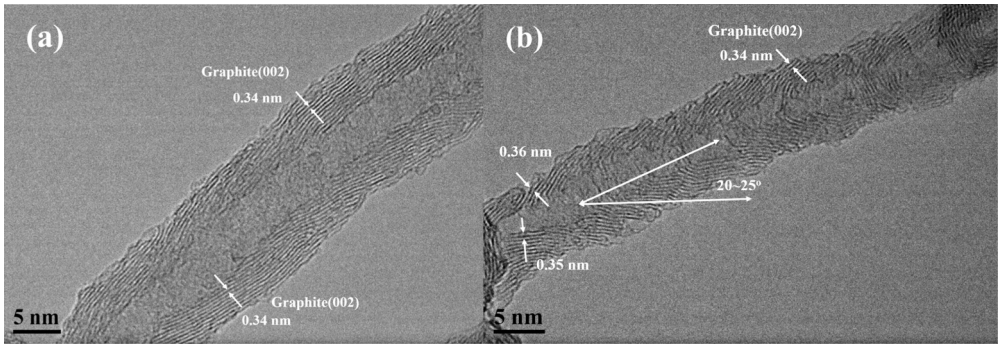

Fig. 7. HRTEM graphs of typical CNTs obtained from PP/PP-MAH/OMMT/Ni–Al: (a) Ni/Al = 9/1 and (b) Ni/Al = 7/3.

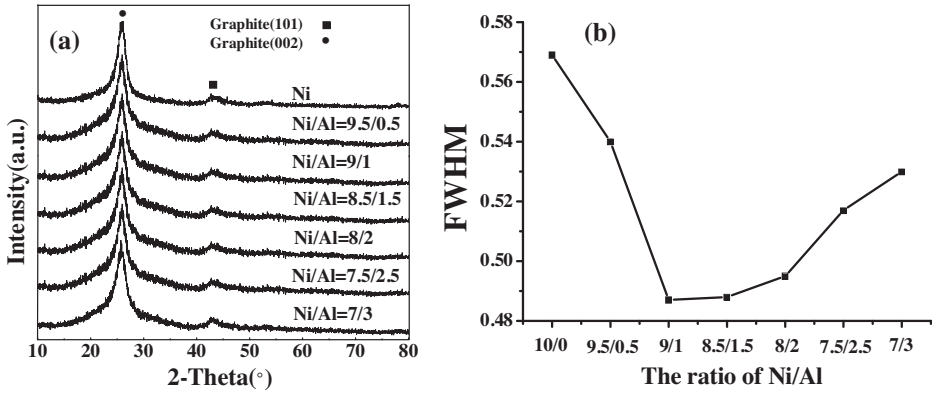

Fig. 8. XRD patterns (a) and the obtained FWHM (b) of MWCNTs with purification from PP/PP-MAH/$_5$OMMT/$_5$Ni–Al mixtures at 1073 K.

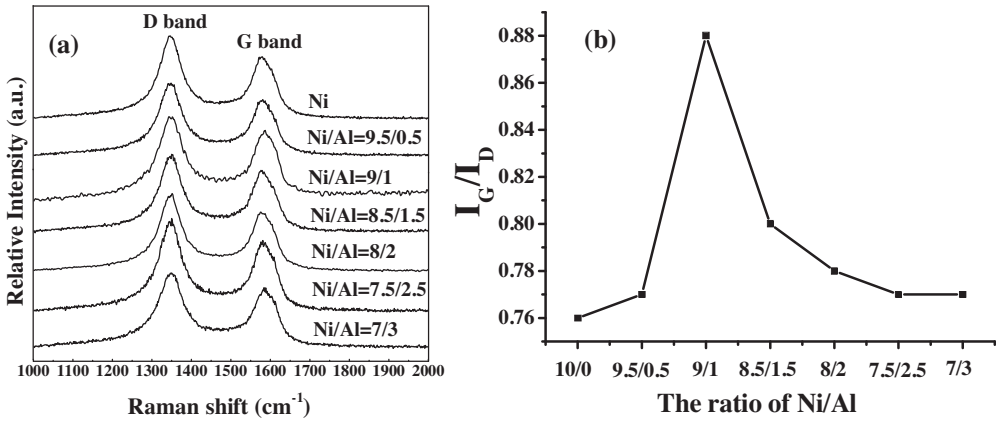

Fig. 9. Raman spectra (a) and I_G/I_D of MWCNTs with purification from PP/PP-MAH/$_5$OMMT/$_5$Ni–Al mixtures at 1073 K.

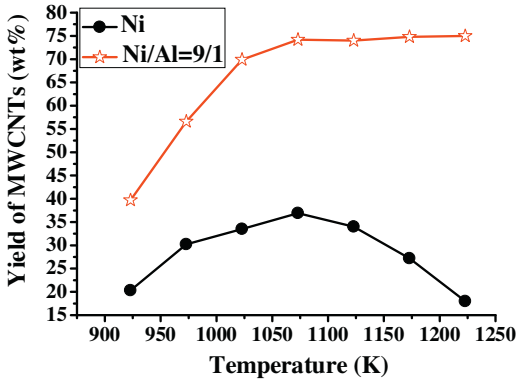

Fig. 10. The effect of temperature on the yield of MWCNTs from PP/PP-MAH/10OMMT/5Ni–Al (Ni/Al = 9/1) and PP/PP-MAH/$_{10}$OMMT/$_5$Ni.

The addition of Al increased the surface area of Ni catalyst (~28.65 $m^2 g^{-1}$ versus 2.33 $m^2 g^{-1}$), which ensured a good dispersion of the active metal and consequently higher catalytic activity.

Finally, as displayed in Fig. 10, the yield of MWCNTs catalyzed by Ni catalyst firstly increased to reach the maximum at 1073 K and then declined with rising temperature. In contrast, Ni–Al catalyst showed different trends. The yield of MWCNTs gradually increased at first but stagnated as the temperature was further increased. Two curves in Fig. 10 reflect that Al could remarkably improve the thermal stability of the catalyst, resulting in a wider range of reaction temperature s where the catalyst does not suffer deactivation during the reaction time. The above reasons may explain why the addition of Al could enhance the catalytic activity of Ni catalyst.

Another intriguing question question was that why the Ni/Al molar ratio remarkably influence the morphology and graphitization of the resultant MWCNT. As shown by TPR curves in Fig. 3, reduction peaks of Ni–Al bimetallic sample shifted to higher temperature was due to the increase of the NiO–Al_2O_3 interaction when the ratio of Ni/Al increased. Gong et al. [49] investigated the influence of NiO catalyst diameter on the yield, morphology, microstructure of CNTs. When the diameter of NiO catalyst increased from 18 to 227 nm, the yield of CNTs almost linearly decreased from 51.9 to 10.8 wt%. And they found that NiO catalysts with small diameter facilitated the growth of long and straight CNTs, while NiO catalysts with large diameter (e.g., 227 nm) favored the formation of short and surface-rugged CNTs. And the coalescence and reconstruction of NiO particles happened during the growth of CNTs. In our system, the interaction between Ni species and amorphous Al_2O_3 was the main difference compared with their system. Although the diameter of NiO (or Ni) changed a little with the Ni/Al ratio, the interaction between Ni species and amorphous Al_2O_3 became stronger when the ratio of Ni/Al decreased. The NiO–Al_2O_3 interaction was of crucial importance because it facilitated particle attachment and stabilization during the growth of CNTs, which in turn affected the morphology of CNTs. The interaction will prevent the catalyst particles from the agglomeration. Steplewska and Borowiak-Palen [50] found that the strong interaction between iron particles and MgO (support) led to the decrease of the catalyst particles active in the formation of CNTs. And weak interaction between Pt and MgO led to sintering during the growth of CNTs. The interaction of catalyst and support had striking influence on the diameter of catalyst particles during the growing process, thus affecting the final diameter of obtained CNTs. In our system, the interaction between Ni species and amorphous Al_2O_3 became stronger when the ratio of Ni/Al decreased from 9/1 to 7/3. Consequently, the diameter during the growth of CNTs decreased, and then the diameter of CNTs showed a decreasing trend. Moreover, when the interaction between Ni species and amorphous Al_2O_3 was strong, the diffusion length was relatively short and hence carbon atoms may not be supplied uniformly over the whole region of the particles. Therefore, the obtained CNTs became shorter when the ratio of Ni/Al decreased from 9/1 to 7/3. And due to strong NiO–Al_2O_3 interaction, there was less chance to form a nucleation seed and more chance to form defects on tube walls. So the graphitization of CNTs decreased when the ratio of Ni/Al decreased from 9/1 to 7/3.

4. Conclusion

In summary, the introduction of Al as a promoter to the Ni catalyst led to better crystallographic properties and superior catalytic activities for the preparation of MWCNTs. Because of the interaction between Ni species and amorphous Al_2O_3, the addition of Al gave rise to an increased surface area and improved stability, with an associated decrease in sizes of Ni particles. The reduction temperature for Ni on bimetallic Ni–Al catalyst was also increased when compared with the monometallic Ni catalyst. The bimetallic Ni–Al catalyst displayed a significant enhancement in the yield of MWCNTs, almost twice of that of monometallic Ni catalyst. The composition of Ni/Al has a significant influence on the yield, morphology and graphitization of MWCNTs. When the addition of Al was 10%, the yield of MWCNTs was the highest, and the thus-obtained MWCNTs had the highest graphitization and minimum amount of defects. The addition of higher amount of Al resulted in a decrease both in yield and graphitization of MWCNTs. We found the best composition of Ni–Al bimetallic catalyst with the best catalytic activity. Given that the introduction of Al to Ni monometallic catalysts can not only decrease the content of the expensive metal Ni—but simultaneously improve the properties (such as the improved catalytic activity and enhanced stability), the Ni–Al bimetallic catalyst is a promising alternative to the traditional monometallic Ni catalyst for preparation of MWCNTs from PP.

References

[1] S. Iijima, Nature 354 (1991) 56.
[2] D.A. Gomez-Gualdron, J.M. Beetge, J.C. Burgos, P.B. Balbuena, J. Phys. Chem. C 117 (2013) 10397.
[3] Y. Shen, A.C. Lua, Appl. Catal. B-Environ. 164 (2015) 61.
[4] G. Wang, H. Wang, Z.X. Tang, W.L. Li, J.B. Bai, Appl. Catal. B-Environ. 88 (2009) 142.
[5] J.B. In, C.P. Grigoropoulos, A.A. Chernov, A. Noy, Acs Nano 5 (2011) 9602.
[6] T.C. Cheng, Mater. Chem. Phys. 136 (2012) 140.
[7] P.G. Savva, K. Polychronopoulou, V.A. Ryzkov, A.M. Efstathiou, Appl. Catal. B-Environ. 93 (2010) 314.
[8] S.K. Youn, C.E. Frouzakis, B.P. Gopi, J. Robertson, K.B.K. Teo, H.G. Park, Carbon 54 (2013) 343.
[9] M. Perez-Cabero, I. Rodriguez-Ramos, A. Guerrero-Ruiz, J. Catal. 215 (2003) 305.
[10] Y. Qin, Q. Zhang, Z.L. Cui, J. Catal. 223 (2004) 389.
[11] A. Bazargan, G. McKay, Chem. Eng. J. 195 (2012) 377.
[12] C.W. Zhuo, Y.A. Levendis, J. Appl. Polym. Sci. 131 (2014) 39930.
[13] J. Gong, J. Liu, Z. Jiang, X. Chen, X. Wen, E. Mijowska, T. Tang, Appl. Catal. B-Environ. 152–153 (2014) 289.
[14] C.W. Zhuo, B. Hall, H. Richter, Y. Levendis, Carbon 48 (2010) 4024.
[15] N. Mishra, G. Das, A. Ansaldo, A. Genovese, M. Malerba, M. Povia, D. Ricci, E. Di Fabrizio, E. Di Zitti, M. Sharon, M. Sharon, J. Anal. Appl. Pyrol. 94 (2012) 91.
[16] J. Gong, J. Liu, Z. Jiang, J. Feng, X. Chen, L. Wang, E. Mijowska, X. Wen, T. Tang, Appl. Catal. B-Environ. 147 (2014) 592.
[17] J. Gong, J.D. Feng, J. Liu, Z.W. Jiang, X.C. Chen, E. Mijowska, X. Wen, T. Tang, Chem. Eng. J. 248 (2014) 27.
[18] J. Gong, J. Liu, L. Ma, X. Wen, X. Chen, D. Wan, H. Yu, Z. Jiang, E. Borowiak-Palen, T. Tang, Appl. Catal. B-Environ. 117–118 (2012) 185.
[19] H.O. Yu, Z.W. Jiang, J.W. Gilman, T. Kashiwagi, J. Liu, R.J. Song, T. Tang, Polymer 50 (2009) 6252.
[20] T. Tang, X.C. Chen, X.Y. Meng, H. Chen, Y.P. Ding, Angew. Chem. Int. Ed. 44 (2005) 1517.
[21] J.A. Rodriguez, Prog. Surf. Sci. 81 (2006) 141.
[22] B.C. Miranda, R.J. Chimentao, J. Szanyi, A.H. Braga, J.B.O. Santos, F. Gispert-Guirado, J. Llorca, F. Medina, Appl. Catal. B-Environ. 166 (2015) 166.
[23] M.H. Amin, K. Mantri, J. Newnham, J. Tardio, S.K. Bhargava, Appl. Catal. B-Environ. 119 (2012) 217.
[24] M.S. Fan, A.Z. Abdullah, S. Bhatia, Appl. Catal. B-Environ. 100 (2010) 365.
[25] M. Zhao, T.L. Church, A.T. Harris, Appl. Catal. B-Environ. 101 (2011) 522.
[26] A. Doner, I. Karci, G. Kardas, Int. J. Hydrog. Energy 37 (2012) 9470.
[27] J.M. Garcia-Vargas, J.L. Valverde, J. Diez, P. Sanchez, F. Dorado, Appl. Catal. B-Environ. 164 (2015) 316.
[28] D. Dutta, R.M. Sankaran, V.R. Bhethanabotla, Chem. Mater. 26 (2014) 4943.
[29] A. Gutierrez-Alejandre, G. Laurrabaquio-Rosas, J. Ramirez, G. Busca, Appl. Catal. B-Environ. 166 (2015) 560.
[30] Z.X. Yu, L.E. Fareid, K. Moljord, E.A. Blekkan, J.C. Walmsley, D. Chen, Appl. Catal. B-Environ. 84 (2008) 482.
[31] L. Kepinski, B. Stasinska, T. Borowiecki, Carbon 38 (2000) 1845.
[32] A.C. Lua, H.Y. Wang, Appl. Catal. B-Environ. 156 (2014) 84.
[33] R.G. Kukushkin, O.A. Bulavchenko, V.V. Kaichev, V.A. Yakovlev, Appl. Catal. B-Environ. 163 (2015) 531.
[34] M.Q. Zhao, Q. Zhang, J.Q. Huang, J.Q. Nie, F. Wei, Carbon 48 (2010) 3260.
[35] C. Wu, P.T. William, Appl. Catal. B-Environ. 90 (2009) 147.
[36] C.F. Wu, P.T. Williams, Appl. Catal. B-Environ. 96 (2010) 198.
[37] M.E. Rivas, J.L.G. Fierro, R. Guil-Lopez, M.A. Pena, V. La Parola, M.R. Goldwasser, Catal. Today 133 (2008) 367.
[38] H.J. Wu, G. Pantaleo, V. La Parola, A.M. Venezia, X. Collard, C. Aprile, L.F. Liotta, Catal. Today 156 (2014) 350.

[39] H.G. Zhang, H. Wang, A.K. Dalai, Appl. Catal. A-Gen. 339 (2008) 121.
[40] T. Belin, F. Epron, Mater. Sci. Eng. B-Adv. 119 (2005) 105.
[41] V. Georgakilas, D. Gournis, M.A. Karakassides, A. Bakandritsos, D. Petridis, Carbon 42 (2004) 865.
[42] T. Tsoufis, L. Jankovic, D. Gournis, P.N. Trikalitis, T. Bakas, Mater. Sci. Eng. B-Adv. 152 (2008) 44.
[43] Z.W. Jiang, R.J. Song, W.G. Bi, J. Lu, T. Tang, Carbon 45 (2007) 449.
[44] R.J. Song, Z.W. Jiang, W.G. Bi, W.X. Cheng, J. Lu, B.T. Huang, T. Tang, Chem.-Eur. J. 13 (2007) 3234.
[45] S. Helveg, C. Lopez-Cartes, J. Sehested, P.L. Hansen, B.S. Clausen, J.R. Rostrup-Nielsen, F. Abild-Pedersen, J.K. Norskov, Nature 427 (2004) 426.
[46] S. Hofmann, R. Sharma, C. Ducati, G. Du, C. Mattevi, C. Cepek, M. Cantoro, S. Pisana, A. Parvez, F. Cervantes-Sodi, A.C. Ferrari, R. Dunin-Borkowski, S. Lizzit, L. Petaccia, A. Goldoni, J. Robertson, Nano Lett. 7 (2007) 602.
[47] H. Yoshida, S. Takeda, T. Uchiyama, H. Kohno, Y. Homma, Nano Lett. 8 (2008) 2082.
[48] D. Chen, K.O. Christensen, E. Ochoa-Fernandez, Z.X. Yu, B. Totdal, N. Latorre, A. Monzon, A. Holmen, J. Catal. 229 (2005) 82.
[49] J. Gong, J. Liu, X.C. Chen, Z.W. Jiang, X. Wen, E. Mijowska, T. Tang, RSC Adv. 4 (2014) 33806.
[50] A. Steplewska, E. Borowiak-Palen, J. Nanopart. Res. 13 (2011) 1987.